FATIGUE CRACK GROWTH BEHAVIOR OF FERRITIC AND AUSTENITIC BUTT-WELDED JOINTS

G. Nicoletto*

A comparative study of the fatigue crack growth performances of austenitic and ferritic-pearlitic weld metals was conducted by testing 20-mm-thick butt-welded joints. Some specimens were tested in the as-welded condition, while others underwent a post-weld heat-treatment. For these multi-pass welded joints, conservative fatigue crack growth rate data are obtained with post-weld heat-treated specimens.

INTRODUCTION

Fatigue failures of transverse butt-welded joints loaded in tension or bending normally initiate at points of geometric stress concentrations provided by weld toes, (1). A simple method of improving the fatigue performance of the joint is to machine the reinforcement flush with the plate surface. Failure then occurs in the weld metal initiated at small, otherwise less important, weld defects. In some recent bending fatigue tests on butt-welded joints with reinforcements machined flush, this author traced the fracture origin back to near-surface or surface-breaking porosity such as that shown in Fig. 1. The quasi-spherical shape of a pore caused by gas entrapped during solidification provided a geometrical stress concentration which strongly affected the fatigue resistance of the welded joint by accelerating crack initiation.

This paper deals with a comparative study of the fatigue crack growth (FCG) properties of austenitic and ferritic weld materials. Multi-pass butt-welded joints were tested at different stress ratios in four-point-bending with edge cracks propagating in the short-transverse direction. As residual stresses affect the fatigue performance of as-welded joints,(1-4), FCG rates were also obtained with post-weld heat-treated specimens.

* DIEM, University of Bologna, Viale Risorgimento,2, Bologna, Italy

MATERIALS AND EXPERIMENTAL PROCEDURE

The welded joints used in this investigation were obtained by butt-welding 20-mm-thick annealed metal plates by the gas metal-arc (GMA) welding process. The weld direction was parallel to the plate rolling direction. A semi-automatic multi-pass technique was used with a equal double-V groove preparation. Details are given in (5). Weld beads were deposited alternatively on either side of the joint to limit warping. Test specimens were obtained by machining out 10-mm-thick bars according to the scheme of Fig. 2. Two weld materials were studied: a C-Mn-Si (ferritic) steel (Electrode trade name: ESAB OK AUTROD 12.51 DIN 3559 SG2-AWS A/SFA 5.18: ER 705) and a stainless (austenitic) steel (Electrode trade name: BOEHLER A7 DIN 8575 - AWS E8-200 zrkn.). Nominal chemical compositions and mechanical properties are summarized in Tab. 1.

Fatigue cracks were propagated from through-the-thickness starter notches centered in the weld by cyclic four-point-bending at room temperature. All tests were carried out on a 150 kN servo-hydraulic testing machine operated in load-control at 15 Hz. Crack length was monitored optically under 50X magnification. Stress intensity factors were computed using the recommended formula to the 4PB specimen geometry. Crack growth rates were computed according to the ASTM E 647-84 incremental seven point method. For both types of welded joints, a part of the specimens were tested in the as-welded (AW) condition, while others underwent a post-weld heat-treatment (PWHT) of 1 hour at 650°C and slow cooling to room temperature designed to relieve residual stresses.

Vickers hardness distributions in the short-transverse direction were preliminarely obtained to characterize the material inhomogeneity in the joints due to multi-pass weld deposition. Significant hardness variations with depth are observed in the compound plot of Fig.3 and are attributed to the local heat treatment applied by sequential weld deposition. The trends for both materials are similar. The different material responses encountered during crack propagation may affect FCG rates.

RESULTS

Ferritic Material

The characterization of the AW joints was performed at two different stress ratios (namely, R = 0.1 and 0.4) as shown in Fig. 4 where the FCG rates data are plotted against the stress-intensity factor range. An asymmetry of the resulting residual stress pattern about the weld mid-thickness was expected because of the limited number of passes with deposition on opposite sides of the joint. Therefore data were obtained at R=0.1 with specimens having starter

notches on opposite sides of the weld to reveal a directional effect on crack propagation and are shown in Fig. 4.

The effect of a PWHT on the present multi-pass butt-welded joints was investigated for R = 0.1 as shown in Fig. 5. When compared to the AW state, the data of the stress-relieved joints are shifted upward in the (da/dN vs. Delta K) plot.

Austenitic Material

Similar tests were performed on the austenititc material. AW joints were tested at two different R-ratios (namely, R = 0.1 and 0.48) as shown in Fig. 6. The effect of a PWHT on the present multi-pass butt-welded joints was investigated for R = 0.1 as shown in Fig. 7. When compared to the AW state, the data of the stress-relieved joints are shifted upward in the (da/dN vs. Delta K) plot implying a reduced resistance to crack extension. The FCG rate data at R=0.1 obtained with AW specimens having starter notches on opposite sides of the weld are also shown Fig. 7. It is worth noting that the FCG rates in this material show irregularities with ΔK which resemble the trend of the hardness distribution of Fig. 3.

DISCUSSION

Since previous studies such as (3) already showed that locus of crack path (weld metal or heat-affected-zone), welding process and heat input do not affect strongly the FCG rate response, the present discussion focuses primarely on effects of stress ratio and PWHT on the present weld materials. Inevitably the interpretations largely, although qualitatively, resorts to the expected influences of residual stresses on FCG rates.

Stress ratio

In a previous study, (5), an insensitivity to positive stress ratios of the mild steel base material when tested with the present specimen geometry was attributed to the absence of significant plasticity-induced crack closure caused by the prevailing plane strain condition and the bending specimen geometry. The stress ratio effect in the AW ferritic joints of Fig. 4 can therefore be attributed mainly to the residual stresses which develop in the transverse direction. The AW austenitic joints of Fig. 6, on the other hand, appear less influenced. By resorting to the superposition principle presented by Parker in (2), similar trends in the data were explained in (5) in terms of a compressive residual stress intensity factor acting at the crack tip. For an edge crack, it would imply either a compressive residual stress on the surface or strong gradients which turn tensile residual stresses on the surface to compressive residual stresses immediately below.

PWHT

Although sometimes recommended, the effectiveness of a PWHT as a fatigue improving factor is still debated and apparently is welded-joint-configuration-dependent, (2,5). Furthermore, evidence such as that of (2) indicates that PWHT can deteriorate the performance of a joint when welding residual stresses are compressive. This is apparently the case for the present butt-welded joints and the short transverse direction of crack growth as shown in Figs. 5 and 7. Interestingly, FCG rates obtained with AW and PWHT ferritic joints tend to coalesce at high ΔK because residual stress effects vanish as crack grows. On the other hand, the observed shift in the data for AW and PWHT austenitic joints could be due to a simultaneous change in residual stress and in the mechanisms of crack propagation.

Material

Comparisons of the present results with FCG rate data for other directions of crack growth in austentitic, (4), and ferritic , (6), butt-welded joints reveal appreciably similar behaviors. On the other hand, while the responses to a PWHT of the weld materials tested here are similar as demonstrated by Figs. 5 and 7, a change in stress ratio produces different responses as depicted in Fig. 4 and 6. Furthermore, the FCG rates for the austenitic joints are always somewhat higher than the corresponding data for the ferritic joints indicating a superior FCG resistance of the latter material.

REFERENCES

(1) Gurney, T.R., "Fatigue of welded structures", 2nd Ed. Cambridge Univ. Press, 1979

(2) Parker, A.P., "Residual stress effects in fatigue", ASTM STP 776, 1982, pp.13-31

(3) Ohta, A., and others, "Current Research on Fatigue Cracks", T. Tanaka and others Eds., Elsevier Appl. Sc., 1987, pp.181-200

(4) Itoh, Y., and others, Eng. Fract. Mech., Vol.33, 1989, pp.397-407

(5) Nicoletto, G., "Fatigue Crack Propagation in Multipass Welded Joints of Mild Steel", Int. J. Pressure Vessels and Piping, Elsevier, 1990, in press

(6) Moghadan S.P. and J.C. Radon, Procs ICF6, "Advances in Fracture Reasearch", Pergamon Press, 1984, pp. 1999-2006

TABLE 1 - Chemical compositions and mechanical properties of weld materials

	C	Mn	Si (wpc)	Ni	Cr	Tensile strength (MPa)	Elong. (%)	Charpy energy (J)
Austenitic	.15	6	-	8.5	19	620	35	78
Ferritic	.10	1.4	0.8	-	-	500	24	80

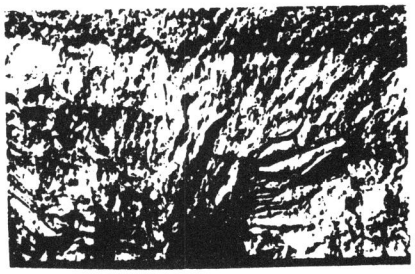

Fig. 1 - Weld porosity

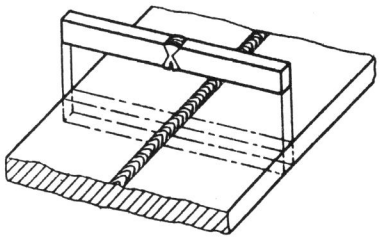

Fig. 2 - Scheme for specimen preparation

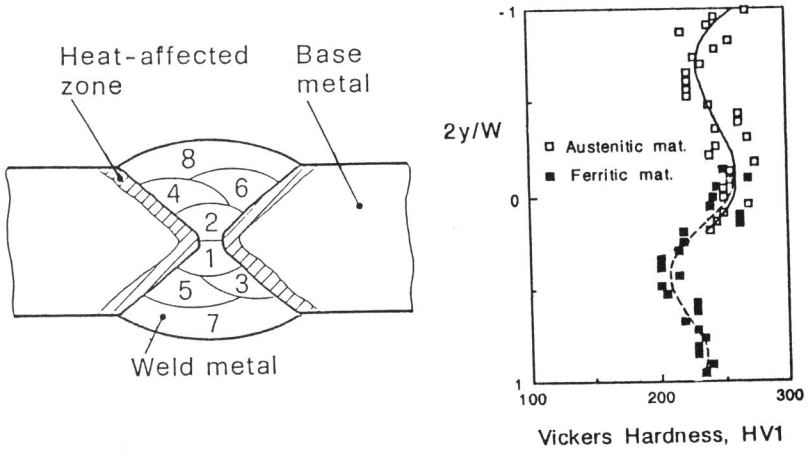

Fig. 3 - Weld deposition sequence for butt-welded joints and hardness distributions in the short-transverse direction

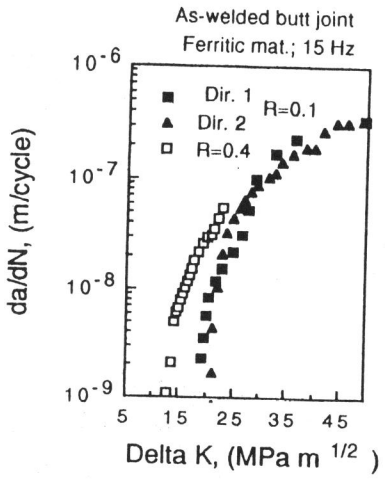

Fig. 4 - Stress ratio effect on FCG rates: Ferritic mat.

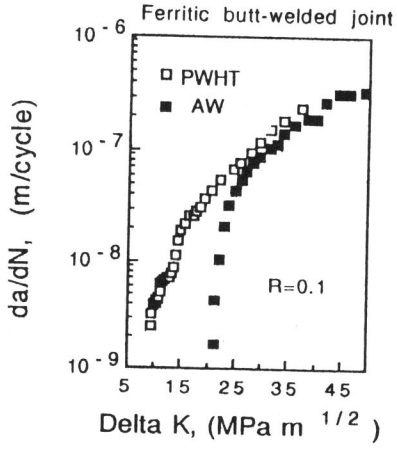

Fig. 5 - PWHT effect on FCG rates : Ferritic mat.

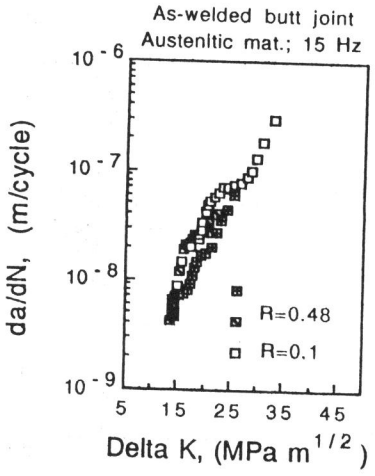

Fig. 6 - Stress ratio effect on FCG rates: Austenitic mat.

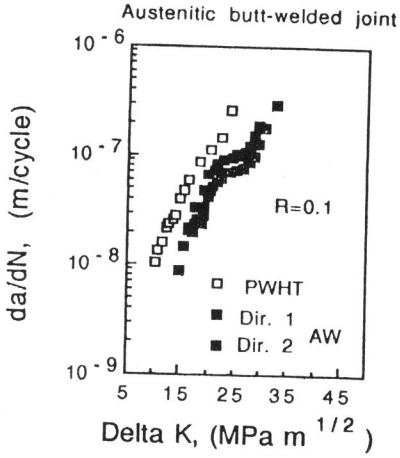

Fig. 7 - PWHT effect on FCG rates : Austenitic mat.